IOP Conf. Series: Journal of Physics: Conf. Series **1256** (2019) 012004 doi:10.1088/1742-6596/1256/1/012004

Round-robin tests of porous disc models

S. Aubrun[1*], M. Bastankhah[2], R.B. Cal[3], B. Conan[1], R.J. Hearst[4], D. Hoek[5], M. Hölling[6], M. Huang[5], C. Hur[5], B. Karlsen[4], I. Neunaber[6], M. Obligado[7], J. Peinke[6], M. Percin[8], L. Saetran[4], P Schito[9], B. Schliffke[1], D. Sims-Williams[2], O. Uzol[8], M.K. Vinnes[4], A. Zasso[9]

[1]Centrale Nantes; LHEEA lab., Nantes, France
[2]Durham University, Durham, United Kingdom
[3]Portland State University, Portland, USA
[4]Norwegian University of Sciences & Technology, Trondheim, Norway
[5]Delft University of Technology, Delft, Netherlands,
[6]Forwind-University of Oldenburg, Oldenburg, Germany,
[7]LEGI Lab., Saint Martin d'Hères, France,
[8]Middle-East Technical University, Ankara, Turkey
[9]Politecnico di Milano, Milano, Italy

Abstract. Nine research teams organized a round-robin measurement campaign of the wake of two porous discs in a homogeneous and "low-turbulent' flow. Mean streamwise velocity and turbulence intensity profiles at four diameters downstream of the discs were measured and compared through such metrics as the maximum of velocity deficit, the maximum of turbulence intensity, the wake width and the thrust coefficient. The dependence of these metrics on the inflow conditions (freestream turbulence intensity and Reynolds number based on the disc diameter) is discussed.

1. Introduction

Following the outcomes of the experts workshop organized by ForWind-Uni Oldenburg in 2018 March 22-23 on Wind Energy Science & Wind Tunnel Experiments, it has been agreed to qualify the smallest wind turbine models (rotor diameter lower than 0.5m) as Wake-Generating Turbine models (WGT). The limitations of small Reynolds numbers and geometrical simplifications result in the improper reproduction of the near flow ($x/D < 3$-4). Studies show that these small models are appropriate to model the far-wake properties [1, 2] and are therefore acceptable, when studying the wake interactions at a wind farm scale [3, 4]. Several concepts of WGT exist (porous discs with different levels of complexity, rotating wind turbines) and have been tested in different facilities. That brings about a variety of results in terms of wake expansion, velocity deficit evolution, turbulence production, etc. Therefore, nine research teams who attended the workshop decided to organize a round-robin measurement campaign to identify the key-elements that can explain these discrepancies.

*Corresponding author : sandrine.aubrun@ec-nantes.fr

The aim of the present round-robin is to rationalize the description of the wake generated downstream of two specific porous disc models by performing similar wake measurements in nine different wind tunnels. The homogeneous incoming flow properties are carefully documented and the wake properties are compared in terms of mean velocity and turbulence intensity profiles at four rotor diameters downstream of the porous discs.

The measurements conducted in these round-robin tests are presented herein. The comparison between the mean velocity profiles and the turbulence intensity profiles is discussed and discrepancies are interpreted through the analysis of the inflow condition properties (primarily Reynolds number and freestream turbulence intensity).

2. Experimental set-ups

2.1. Porous disc models

The two selected models are based on the simplest wind turbine model, which is the actuator disc concept. *Disc A* is a porous disc made of metallic mesh with a uniform porosity of 57% and a disc diameter of 200mm [2] and *Disc B* is a porous disc made of plywood with a radially non-uniform porosity and a disc diameter of 120mm [3] (Fig. 1). Both discs are fixed to a rod of 10mm of diameter, reproducing the wind turbine tower. The top of the rod is fixed to the center of the disc.

The spatial axes (x, y, z) are orientated so that x is the streamwise component, y points in the lateral direction and z is the vertical component. The reference framework is centred on the discs center.

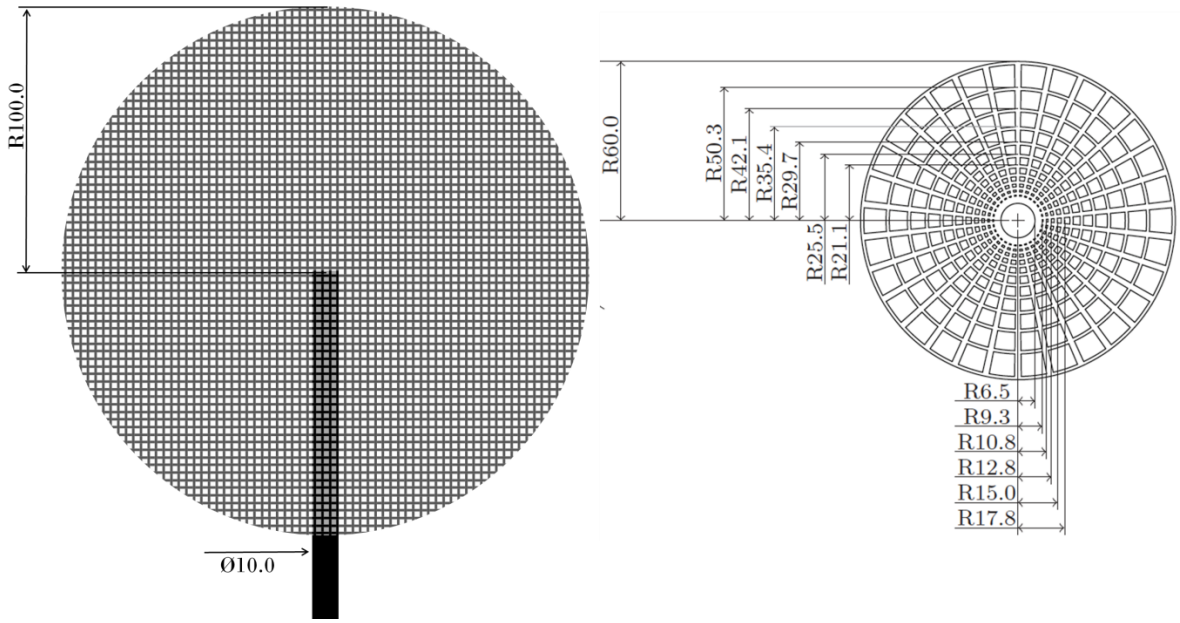

Figure 1: Geometric properties of the porous discs tested in the round-robin. *Disc A*: Uniform porous disc (left, [2]) and *Disc B*: non-uniform porous disc (right, [3])

Velocity measurements within the wake of both models have been performed in nine facilities operated by Durham University (DURHAM), Centrale Nantes (ECN), LEGI-CNRS (LEGI), Middle-East Technical University (METU), Norwegian University of Science & Technology (NTNU), Delft University of Technology (TUDELFT), Politecnico di Milano (POLIMI), Portland State University (PSU) and ForWind-University of Oldenburg (UOLD).

2.2. DURHAM facility

The Durham University 2m2 Wind Tunnel is a ¾ open jet Eiffel-type wind tunnel. The contraction is 8:1 including bellmouth (4:1 from screens), and the air jet speed in the test section can vary from 0 to 30 m/s. Further details are available in [5, 6]. A particular capability of the tunnel (albeit not used here) is an active system for the generation of transient flows [7]. Velocity measurements were performed with a five-hole pressure probe, built and calibrated in-house and measurement repeatability was confirmed to be within 1% for the results presented here.

2.3. ECN facility

Experiments were conducted in the boundary-layer wind tunnel of the Laboratoire de recherche en Hydrodynamique, Energétique et Environnement Atmosphérique of Ecole Centrale de Nantes (LHEEA, Nantes, France), which has test-section dimensions of 24m × 2m × 2m. The turbulence intensity is 1.2%. The discs were fixed to a rod which was long enough to ensure that the discs were located in an area where the flow is homogeneous. Blockage ratios created by the discs within the test section are 0.78% and 0.3% for Disc A and Disc B, respectively. Velocity measurements were performed with a Cobra probe; the sampling frequency was 1.25 kHz and the sampling time 600s.

Team	Type of instrumentation	Meas. error [m/s]	dynamic response [kHz]	sampling frequency [kHz]	sampling time [s]	Reference wind speed [m/s]	Reynolds number [10^3]	Freestream turbulence intensity [%]	Integral length scale [mm]	Blockage ratio [%]	rod length [mm]	Disc
DURHAM	Durham University 5-Hole Probe	0.25 max	0.25	4	65	25	333 200	1.5	400	1.6 0.6	300	A B
ECN	Cobra probe	0.3	0.15	1.25	600	4.5 / 6.7	60 / 89 36 / 54	1.2	45.7	0.78 0.3	1000	A B
LEGI	Cobra probe	0.3	0.5	1.25	180	7.0 / 12.0	93 / 160 54 / 95	<0,5	-	5.6 2	375	A B
METU	Single hot wire anemometry	0.23	0.4	10	5	9.0 / 16.9 13.9	100 100 / 200	0.4 / 0.6 0.6	2.7/2.1 2.8	3.15 1.15	500	A B
NTNU	3 single hot wires anemometry	0.1	10	30	300	8	100 62	0.3-0.6	-	2.6 0.9	900 (rod + tower)	A B
POLIMI	Cobra probe	0.3	2	2	30	10 / 20 10 / 20	133 / 266 80 / 160	2	-	8 3	321 292	A B
PSU	2D-2C PIV	0.2	-	0.005	600 (3000 snapshots)	8.3	184 110	0.4	-	3.3 1.2	600 600	A B
TUDELFT	Robotic PIV, tomographic PIV	0.02	-	0.5	10 (5000 snapshots)	5	40	2	-	1.92	500	B
UOLD	Single hot wire anemometry	max 0.13	10	20	20	4.1/6.5/7.5 6.5/7.4/12.5	55 / 89 / 101 53 / 61 / 101	<0.4	-	0.35 0.12	530	A B

Table 1: Experimental conditions of the round-robin

2.4. LEGI facility

Experiments at LEGI were performed in a low-turbulence wind tunnel with a measurement section of 4m long and a square cross-section of 0.75x0.75m². For the two freestream velocities considered, background turbulence (measured via hot-wire anemometry and an empty test section) remains always below 0.5%. The models were placed at 0.5m from the section's inlet and very close to its centre.

Blockage ratios created by the discs within the test section are 5.6% and 2% for Disc A and Disc B, respectively. Horizontal and vertical traverses within the wake are conducted using a Cobra probe and data are acquired for 180s and with a sampling frequency of 1.25 kHz at each traverse point.

2.5. METU facility

METU experiments are conducted at an open-return suction type wind tunnel that has a test section of 1m×1m cross-section. The average inlet turbulence intensity is about 0.5%. The discs are placed at the centre of the wind tunnel, where the flow is most homogeneous. Blockage ratios created by the discs within the test section are 3.15% and 1.15% for Disc A and Disc B, respectively. Horizontal and vertical traverses within the wake are conducted using a single sensor CTA system and data are acquired for 5 s and with a sampling frequency of 10 kHz at each traverse point.

2.6. NTNU facility

The recirculating wind tunnel at NTNU has a test-section that measures 2.7 m x 1.8 m x 12 m (width x height x length). The discs were placed in the centre of the test-section 1.6 m downstream of the inlet. The discs were mounted to a 10 mm pole, which transitioned to a thicker 35 mm pole at a distance of 200 mm from the centre of the disc. The turbulence intensity varied from 0.3% to 0.6% (peak-to-peak) across the test-section. Three single-wire hot-wire probes were driven simultaneously by a Dantec StreamLine Pro constant temperature anemometer. Signals were acquired at 30 kHz for 300 s with an analogue filter at 10 kHz.

2.7. TUDELFT facility

Wind tunnel measurements using robotic volumetric PIV are conducted in the W-Tunnel of the TU Delft Aerodynamic Laboratories. The W-tunnel is an open-jet open-return wind tunnel with a square 0.6m x 0.6m exit. The robotic PIV system consists of three major parts: the coaxial volumetric velocimeter (CVV), comprised of a compact arrangement of four CMOS cameras (10 bits, 800×600 pixels) at low tomographic aperture and an optical fibre delivering the light emitted by a Nd:YLF Quantronix Darwin Duo Laser (21 mJ pulse energy @ 1 kHz, 527 nm wavelength), a robotic arm (Universal Robots UR5) that allows the robotic manipulation of the CVV system with six degrees of freedom, and the helium-filled soap bubbles (HFSB) seeding generator, which delivers sub-millimetre neutrally buoyant tracer particles at a nominal rate of 6×10^6 tracers per second.

2.8. POLIMI facility

The POLIMI wind tunnel is a closed-circuit facility, with a maximum wind speed of 55m/s and test section size 1m x 1.5m (width x height). The freestream turbulence intensity is 2%. Blockage ratios created by the discs within the test section are 8% and 3% for Disc A and Disc B, respectively. Velocity profiles are measured using a 2D traversing system placed 4D downstream and 2 cobra probes are installed at 100mm distance for the measurement of the wake profile.

2.9. PSU facility

The test section of the close-circuit wind tunnel at Portland State University has dimensions of 5m (length), 1.2m (width), and 0.8m (height). The contraction ratio is 9:1. The freestream wind speed may be adjusted in a reliable working range of 2–40 m/s. The freestream turbulence intensity is 0.4%. Particle image velocimetry (PIV) was used to measure the instantaneous velocity fields. A Nd:Yag (532 nm, 1200 mJ, 4 ns duration) double-pulsed laser sheet was generated. The flow was periodically seeded with vaporized di-ethylhexyl-sebacate and the concentration of the seeding was kept at a constant level to ensure consistency of particle imaging. A camera (4MP ImagerProX) was used to collect flow snapshots. The PIV measurement window was approximately 0.2m x 0.2m in the streamwise and spanwise directions. Velocity vectors were calculated using a multi-pass FFT based algorithm with two passes each at 64 and 32 pixel interrogation windows.

2.10. UOLD facility

The experiments at ForWind, University of Oldenburg, have been carried out in the 30 m long closed test section of Oldenburg's Large Wind Tunnel (OLWiT), that has an outlet of 3 m x 3 m [8]. The freestream turbulence intensity is lower than 0.4%. Blockage ratios created by the discs within the test section are 1.3% and 0.5% for Disc A and Disc B, respectively. Data was collected using a Dantec StreamLine with 1D hot-wire anemometry, and the sensor length was 1.25 mm. A hardware low-pass filter with a cut-off frequency of 10 kHz was used, and the sampling frequency was 20 kHz. 4.10^5 data points were collected at each position.

2.11. Experimental conditions

Table 1 summarizes the experimental conditions in each facility. The experiments were performed in a homogeneous freestream flow, outside of any wall effects and with a freestream turbulence intensity as low as possible, depending on the facility constraints. The flow homogeneity was checked by measuring the freestream velocity in the empty test section along a crosswise plane larger than the disc area. The velocity field without the presence of discs can be used to correct any residual inhomogeneity effects in the non-dimensioning of the velocity profiles with the discs. The freestream turbulence intensity across all facilities varies between 0.3% and 2%.

The Reynolds number based on the disc diameter ranges from 36 000 to 333 000, covering one decade.

The turbulent integral length scale is given when possible. It is worthwhile to note that the integral length scale measured in DURHAM facility is particularly large and is associated with low-frequency motions that exist in their 3/4 open-jet wind tunnel.

It was recommended to keep the blockage ratio based on the ratio between the disc diameter and the test section below 5%. Nonetheless, this recommendation could not be achieved in all facilities due to geometrical constraints.

Except TUDELFT and PSU who performed PIV measurements, all the other teams chose pointwise measurements (pressure or hot wire probes). In all set-ups, the measurement error is assessed to be lower than 0.3m/s.

3. Results

A direct data comparison across all facilities is performed by plotting the dimensionless mean streamwise velocity U/U_{ext} (Figure 2a for disc A and 3a for disc B) and turbulence intensity I_u (Figure 2b for disc A and 3b for disc B) profiles at x/D = 4, along the crosswise direction perpendicular to the rod. The dimensionless velocity U/U_{ext} is obtained by dividing the local mean streamwise velocity by a reference velocity measured at a location outside of wake effects. The turbulence intensity $I_u = \sigma_u/U$ is the ratio between the standard deviation and the mean value of the local velocity.

The mean velocity profiles measured downstream of disc A present an area of constant velocity deficit. This is due to the uniformity of the disc porosity. The turbulence intensity profiles present two peaks located at wake borders, where the velocity gradient, and so the turbulence production by shear, is at its maximum. Both distributions show that, in these low-turbulent freestream flows, the wake is still characteristic of the near-wake at 4D downstream of the disc A.

The presence of the rod generates a 3D flow disturbance characterised by an overall downwash [9], than can be different depending on the rod length and on the fixation system. Therefore, the distance between the wall and the disc centre is variable (from 1.5D to 8.3D). Typical crosswise time-average velocity fields are presented in Fig. 4. The vertical downwash due to the rod is clearly visible for disc A, as well as a slight horizontal drift due to a slight shear detected in the NTNU set-up (Fig. 4a). The vertical downwash is less intense for disc B, where the axial induction factor is smaller (Fig. 4b). Consequently, the velocity profiles measured at (z/D = 0, x/D = 4) are not systematically crossing the wakes at the same location. This feature can also explain the scatter in results and particularly the fact that the rod's signature is not always visible in the wake profiles.

The mean velocity profiles measured downstream of disc B present a Gaussian-shape velocity deficit, due to the radially non-uniform porosity of the disc. The turbulence intensity profiles present two maxima, that are less pronounced than for disc A, but illustrate that the wake cannot be considered as a fully far-wake, yet.

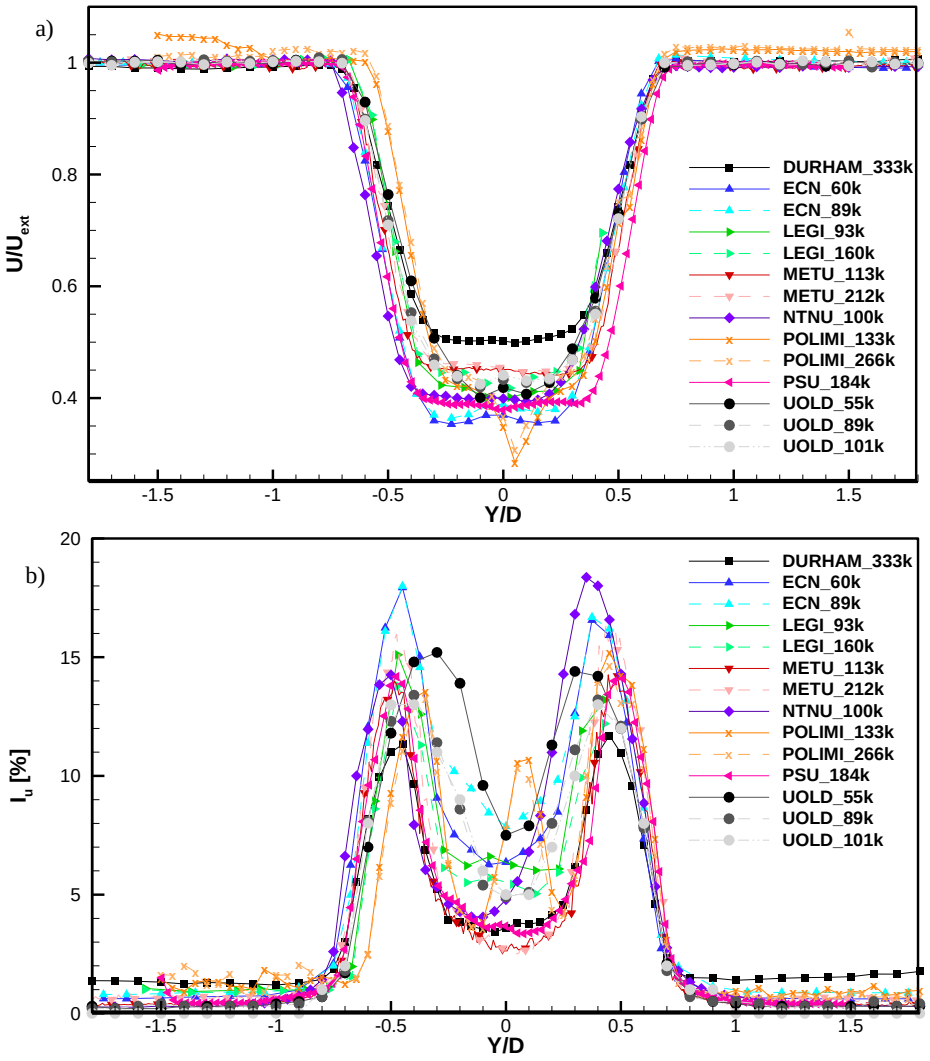

Figure 2: Time-average velocity (a) and turbulence intensity (b) profiles at x/D=4 downstream of the disc A (legends indicate the origin of the data and the Reynolds number based on the disc diameter).

On this first level of comparison, it can be concluded that the obtained results are consistent with each other, even if some slight discrepancies are visible (except for DURHAM results where significant differences with others are observed).

In order to compare the results in more detail, reduced metrics were selected and compared: the maximum of dimensionless velocity deficit $VD/U_{ext} = \left(U_{ext} - min\left(U(y)\right)\right)/U_{ext}$, the maximum of streamwise turbulence intensity $I_{u-max} = max\left(I_u(y)\right)$ the dimensionless wake width $\Delta y/D$, where Δy is the distance between the two crosswise locations where $VD = 0.95$, and the thrust coefficient C_T obtained by applying the momentum theory through integration of the velocity deficit within the wake and up to $VD = 0.95$.

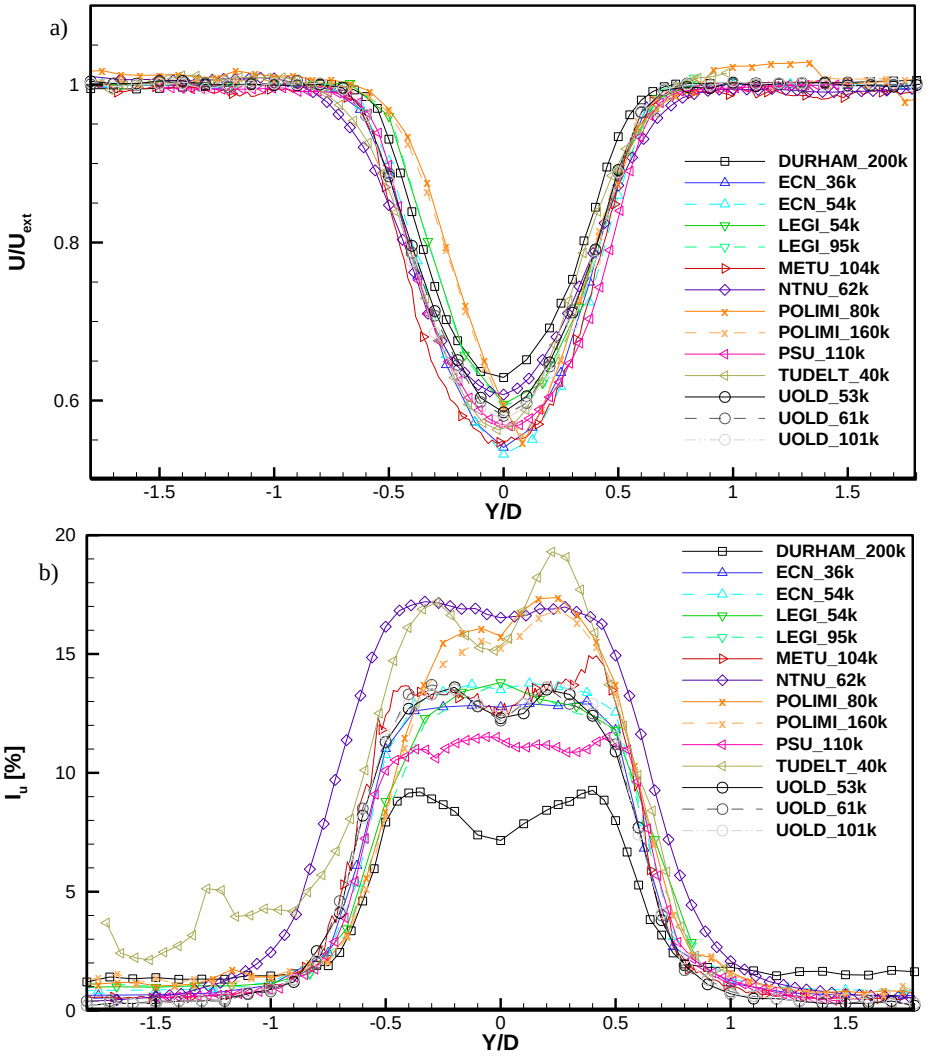

Figure 3: Time-average velocity (a) and turbulence intensity (b) profiles at x/D=4 downstream of the disc B (legends indicate the origin of the data and the Reynolds number based on the disc diameter).

The dependence of these metrics on the freestream turbulence intensity and on the Reynolds number is presented in Figure 5. Clear trends do not appear, but some statements can be drawn.

The dimensionless velocity deficits collapse sufficiently well around 0.6 for disc A and 0.4 for disc B (Fig. 5a). The dependence of this metric on the freestream turbulence intensity cannot be quantified since the scatter is too significant. Reynolds number independence is visible on Fig. 5b. When measurements were performed at several inflow conditions in one facility, no Reynolds effect is detected on the velocity deficit.

The maximum turbulence intensity in the wake varies between 12% and 18% (Fig. 6a). No clear trend can be seen, as the data scatters significantly. Note that, for the majority of results, an opposite distribution between the velocity deficit and the maximum of turbulence intensity is visible. That can be explained by the fact that the larger velocity deficit results in a larger velocity gradient and thus higher turbulence production in wake borders.

A slight dependence (negative trend) of the maximum turbulence intensity on the Reynolds number is visible when measurements are performed at several inflow conditions in one facility (Fig. 6b).

The wake width for disc A does not show any dependence on the freestream conditions or the associated Reynolds number (Fig. 6c and 6d). Except for POLIMI, the wake width is constant at

1.28*D*. This statement is not applicable to disc B, where values vary between 1.05*D* and 1.2*D*. The fact that the velocity deficit of disc B is less pronounced and that the wake borders are less sharp might inhibit the precise determination of the wake borders. When measurements were performed at several inflow conditions in one facility, no Reynolds effect is detected on the wake width.

Following the same trend, the thrust coefficients collapse well for disc A around 0.65 (except for POLIMI) but present more scatter for disc B, with values between 0.33 and 0.51.

DURHAM experiments present quite peculiar results. In particular, the velocity deficit and, by extension, the turbulence intensity are much lower than other results. The only differentiating element of the DURHAM set-up is the particularly large turbulence integral length scale (400mm) in the freestream flow that might generate a wake meandering and explain a mitigation of the mean values.

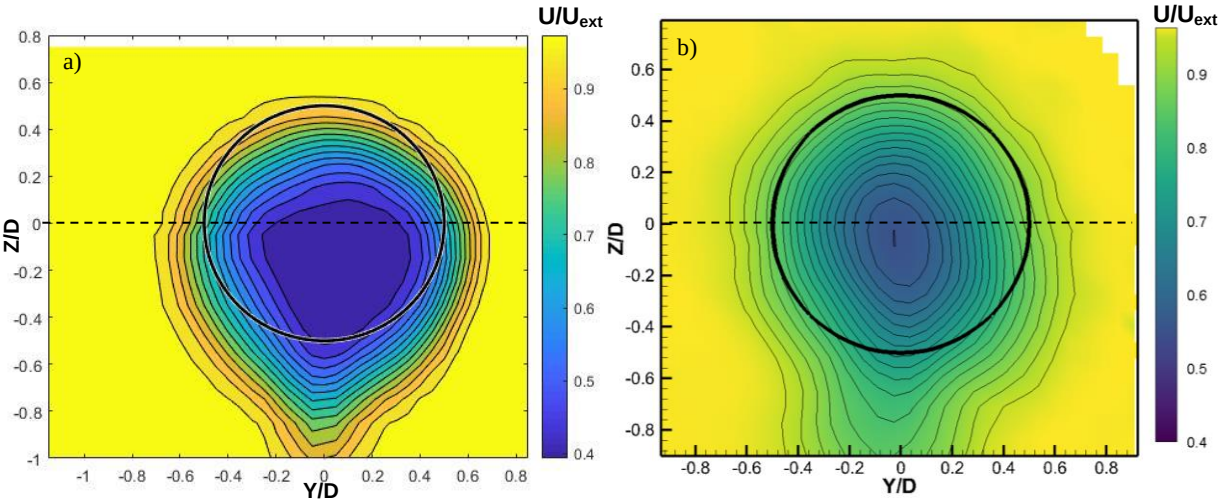

Figure 4: Examples of time-average velocity fields at x/D=4 downstream of the disc a) A (NTNU) and b) B (TU DELFT)

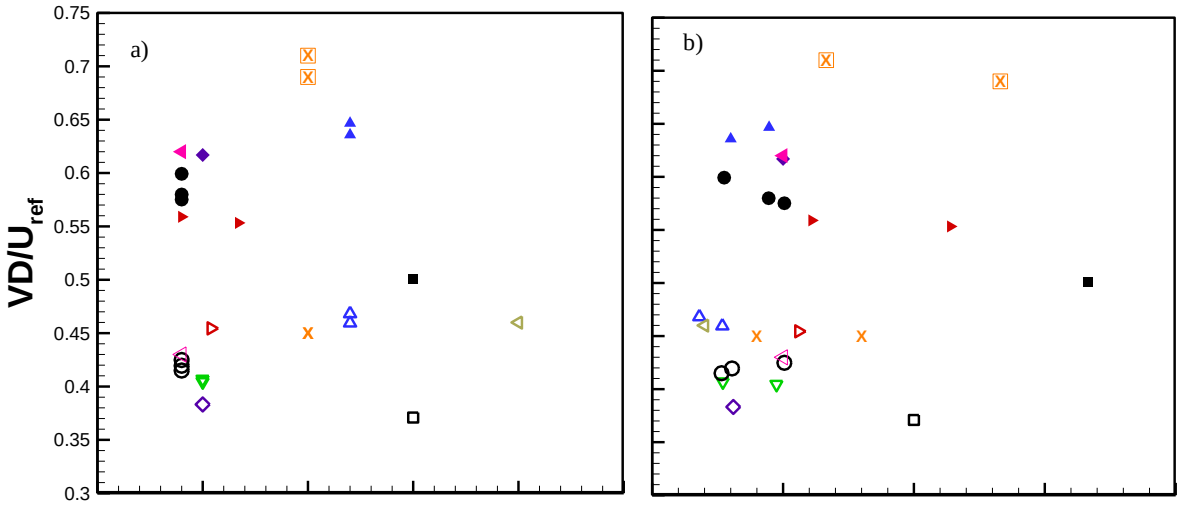

Figure 5: Maximum of velocity deficit (a and b) versus the freestream turbulence intensity (left) and versus Reynolds number based on the disc diameter (right) for disc A (filled symbols) and disc B (empty symbols). ■ Durham, ▲ ECN, ▼ LEGI, ► METU, ♦ NTNU, ☒ POLIMI, ◄ PSU, ◄ TUDELFT, ● UOLD.

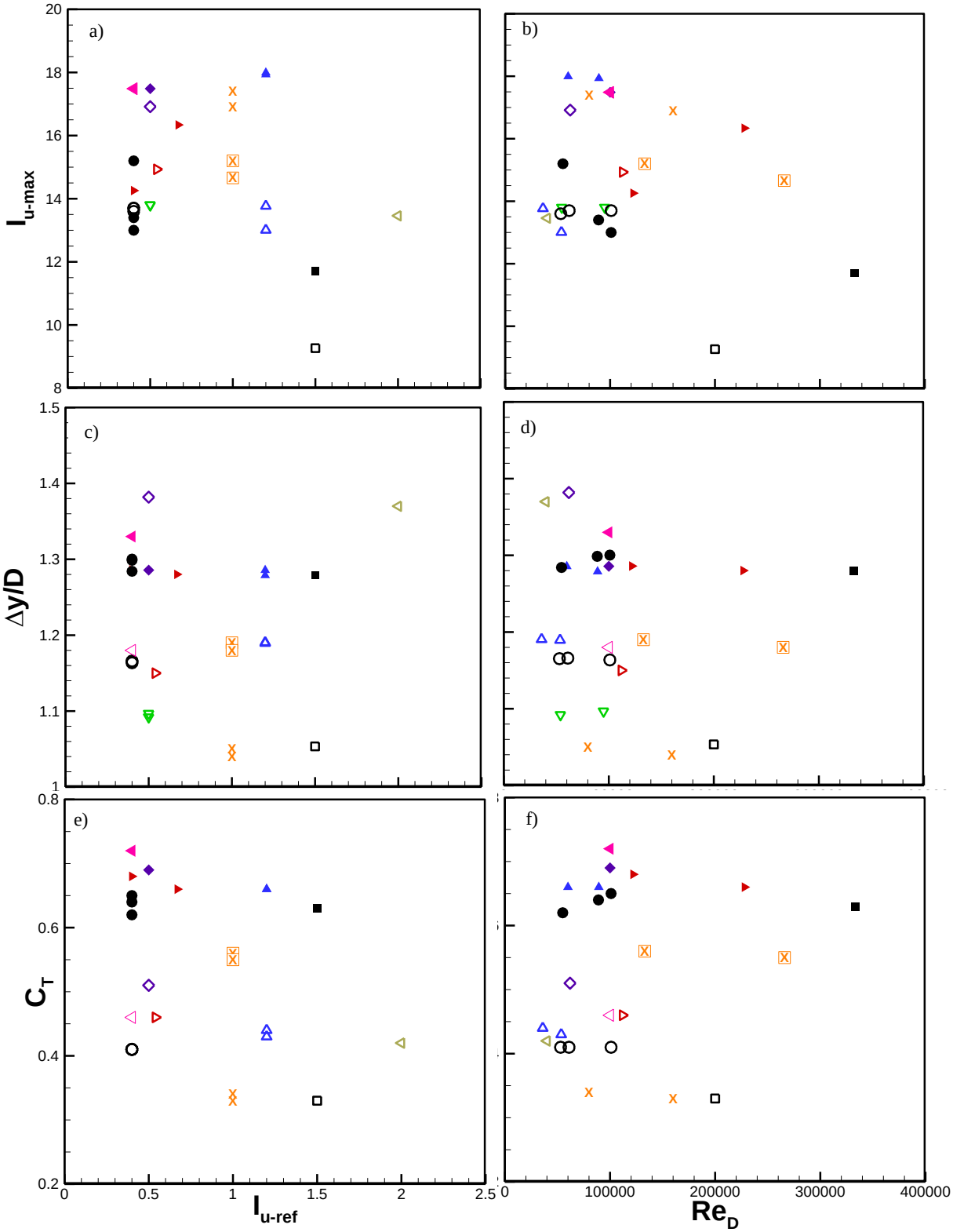

Figure 6: Maximum of turbulence intensity (a and b), wake width (c and d) and thrust coefficient (e and f) versus the freestream turbulence intensity (left) and versus Reynolds number based on the disc diameter (right) for disc A (filled symbols) and disc B (empty symbols). ■ Durham, ▲ ECN, ▼ LEGI, ► METU, ♦ NTNU, ☒ POLIMI, ◄ PSU, ◄ TUDELFT, ● UOLD.

4. Conclusion

Nine research teams organized a round-robin measurement campaign of the wake of two porous discs in a "low-turbulent' homogeneous flow. Mean streamwise velocity and turbulence intensity profiles at four diameters downstream of the discs were measured with classical flow measurement systems (PIV, hot-wire anemometry and multi-hole unsteady pressure probes) and compared through metrics such as the maximum velocity deficit, the maximum turbulence intensity, the wake width and the thrust coefficient. The dependence of these metrics on the inflow conditions (freestream turbulence intensity and Reynolds number based on the disc diameter) is also discussed.

In general, results collapse reasonably well across facilities. It is noticed that, even if all participants used the same rod to mimic the wind turbine tower, the discrepancy in rod fixation and distance between the wall and disc center can generate different wake downwash that might explain the slight scatter in the mean velocity and turbulence intensity profiles.

No clear trend can be noticed regarding the dependence on the freestream turbulence intensity. The Reynolds number independence is obvious when measurements were performed at several inflow conditions in one facility.

These preliminary results open the need for additional tests with more realistic - in terms of wind energy applications - freestream turbulence intensities to be able to identify some clear trends into the data. The effect of integral length scale on the turbine wake structure needs also to be further investigated.

References

[1] Vermeer L.J, Sørensen J.N., Crespo A., Wind turbine wake aerodynamics, Prog. Aerosp. Sci. (2003) 39: 467–510

[2] Aubrun S., Loyer S., Hancock P. E., Hayden P., Wind turbine wake properties: Comparison between a non-rotating simplified wind turbine model and a rotating model, Journal of Wind Eng. and Ind. Aerodyn. (2013) 120:1-8

[3] Camp E. H. Cal R.C., Mean kinetic energy transport and event classification in a model wind turbine array versus an array of porous disks: Energy budget and octant analysis, Phys. Rev. Fluids 1 (2016), 044404

[4] Bossuyt J, Michael F. Howland, MF, Meneveau C, Meyers J, Measurement of unsteady loading and power output variabilityin a micro wind farm model in a wind tunnel Exp Fluids (2017) 58:1

[5] Sims-Williams, DB, Dominy, RG, The Design of an Open-Jet Wind Tunnel for Model Testing, SAE Paper 2002-01-3340, SAE Motorsports Engineering Conference, Indianapolis (2002).

[6] Sims-Williams, DB, Dominy, RG, The Design of a New Wind Tunnel for Vehicle Aerodynamics Research, MIRA Vehicle Aerodynamics Conference, Warwick, UK, Oct. 2002.

[7] Mankowski, O., Sims-Williams, D., and Dominy, R., A Wind Tunnel Simulation Facility for On-Road Transients, SAE International Journal of Passenger Cars - Mechanical Systems 7(3):1087-1095, 2014.

[8] Kröger L, Frederik J, van Wingerden JW, Peinke J, Hölling M (2018). "Generation of user defined turbulent inflow conditions by an active grid for validation experiments." Journal of Physics: Conference Series, 1037. URL http://stacks.iop.org/1742-6596/1037/i=5/a=052002.

[9] Pierella F., Saetran L., Wind tunnel investigation on the effect of the turbine tower on wind turbines wake symmetry, Wind Energy (2017) 20: 1753– 1769